

https://dspace.org/

Antiproliferative and apoptotic effects of indonile derivative N2hydroxy5nitrophenyl 4methylphenyl methyl indoline in breast cancer cells

S Palanivel; Akshaya Murugesan; Kumar Subramanian; Olli Yli-Harja; M Kandhavelu

https://hdl.handle.net/10539/36384
WOS

Downloaded from a DSpace repository. https://dspace.org/

European Journal of Pharmacology 881 (2020) 173195

Contents lists available at ScienceDirect

European Journal of Pharmacology

journal homepage: www.elsevier.com/locate/ejphar

Full length article

Antiproliferative and apoptotic effects of indole derivative, N-(2-hydroxy-5-nitrophenyl (4′-methylphenyl) methyl) indoline in breast cancer cells

Suresh Palanivel[a,b], Akshaya Murugesan[a,b,c], Kumar Subramanian[d], Olli Yli-Harja[b,e,f], Meenakshisundaram Kandhavelu[a,b,*]

[a] Molecular Signaling Lab, Faculty of Medicine and Health Technology, Tampere University and BioMediTech, Tays Cancer Center, Tampere University Hospital, P.O. Box 553, 33101, Tampere, Finland
[b] Institute of Biosciences and Medical Technology, Tampere, Finland
[c] Department of Biotechnology, Lady Doak College, Thallakulam, Madurai, 625002, India
[d] Oncology Division, Department of Internal Medicine, Faculty of Health Sciences, University of the Witwatersrand, Private Bag 3, Wits, 2050, Johannesburg, South Africa
[e] Computational Systems Biology Group, Faculty of Medicine and Health Technology, Tampere University and BioMediTech, Tays Cancer Center, Tampere University Hospital, P.O. Box 553, 33101, Tampere, Finland
[f] Institute for Systems Biology, 1441N 34th Street, Seattle, WA, 98103-8904, USA

ARTICLE INFO

Keywords:
Indoline derivatives
Apoptosis
Gene expression
EGFR
Docking
ADME
QSAR

ABSTRACT

Indoline derivatives functions as an inhibitors of epidermal growth factor receptor (EGFR) with the anticancer potential against various cancers. We aim to investigate anti-breast cancer effects and mechanism of action of novel indoline derivatives. Molecular docking of seven indoline derivates with EGFR revealed, *N*-(2-hydroxy-5-nitrophenyl (4′-methylphenyl) methyl) indoline (HNPMI) as the top lead compound. RT-PCR analysis showed the downregulation of PI3K/S6K1 genes in breast cancer cells through the activation of EGFR with HNPMI. This compound found to have higher cytotoxicity than Cyclophosphamide, with the IC_{50} of 64.10 μM in MCF-7 and 119.99 μM in SkBr3 cells. HNPMI significantly reduced the cell proliferation of MCF-7 and SkBr3 cells, without affecting non-cancerous cells, H9C2. Induction of apoptosis was analyzed by Caspase-3 and -9, DNA fragmentation, AO/EtBr staining and flow cytometry assays. A fold change of 0.218- and 0.098- for caspase-3 and 0.478- and 0.269- for caspase-9 in MCF7 and SkBr3 cells was observed, respectively. Caspase mediated apoptosis caused DNA fragmentation in breast cancer cells upon HNPMI treatment. The structural elucidation of HNPMI by QSAR model and ADME-Tox suggests, a bi-molecular interaction of HNPMI-EGFR which is related to antiproliferative and apoptotic activity. The data concludes that, HNPMI-induced the apoptosis via EGFR signaling pathway in breast cancer cells. Thus, HNPMI might serve as a scaffold for developing a potential anti-breast cancer therapeutic agent.

1. Introduction

Breast cancer is ranked as the second most common cancer worldwide. Report from Global statistics found that among the various types of cancers diagnosed, 12% of the patients were reported with breast cancer(Age standardized (World) incidence rates, breast, all ages, 2018). Though there are multiple factors involved in the cause of disease, lifestyle changes and the environmental factors plays a significant role. Prognosis and the overall survival are uncomplimentary, due to the limited treatment response and drug toxicity. Understanding on the heterogeneity of the breast cancer, numerous advances have been made in the treatment (Musa et al., 2018; Tong et al., 2018; Vaiyapuri et al., 2015). One such development is the use of small molecule targeted therapy in combination with standard chemotherapeutic agents. The current treatment regimens include the myriads of newly approved drugs for treating different subtypes of breast cancer. Despite the advanced treatment, lack of potential drugs or combinations, urges to discover the novel drug for inhibiting the proliferation and metastatic properties of the breast cancer cells.

Indole derivatives function as the inhibitor of epidermal growth factor receptor (EGFR) with the anticancer potential. EGFR is one of the well-studied and vital targets identified against breast cancer. EGFR is a mediator of a wide variety of signal transduction events controlling cell proliferation, migration and their survival (Ali and Wendt, 2017). It is

* Corresponding author. Molecular Signaling Lab, Faculty of Medicine and Health Technology, Tampere University and BioMediTech, Tays Cancer Center, Tampere University Hospital, P.O. Box 553, 33101, Tampere, Finland.
E-mail address: meenakshisundaram.kandhavelu@tuni.fi (M. Kandhavelu).

https://doi.org/10.1016/j.ejphar.2020.173195
Received 6 March 2020; Received in revised form 9 May 2020; Accepted 11 May 2020
Available online 21 May 2020
0014-2999/ © 2020 Elsevier B.V. All rights reserved.

found to be overexpressed in majority of the breast cancers(Masuda et al., 2012). Since EGFR is the major signaling mediator for PI3 kinase, Ras-Raf-MAPK, JNK, and PLC(Downward et al., n.d.), the search for the potent EGFR inhibitors is of interest. Recently, we have synthesized numerous indolines and morpholines derivatives and evaluated its effect against different cancers (Doan et al., 2016; Karjalainen et al., 2018; Palanivel et al., 2020b, 2020a). However, the molecular mechanism of action of the HNPMI against breast cancer is not well studied. The present study is focused to reveal the best indoline derivatives based on its potential interaction with bind to EGFR protein. We performed in-silico screening of seven indoline derivatives that profoundly inhibits the growth of cancer cells.

N-(2-Hydroxy-5-Nitrophenyl (4′-Methylphenyl) Methyl) Indoline (HNPMI) was found to have best interaction with EGFR. We also have investigated the effect of HNPMI on downstream pathway genes of EGFR pathway in breast cancer cell lines. Also, the cytotoxicity and apoptotic induction of the HNPMI was found to be promising. QSAR study was performed to compare the structure and its activity relationship. ADME/Tox analysis was done to understand the drug-likeliness property of the HNPMI, which gives an idea about its bioavailability. These studies explore HNPMI as a potent antiproliferative and apoptosis inducer in breast cancer cells.

2. Materials and methods

2.1. Cell lines, materials

The study was aimed to identify the effect of indoline derivatives in inducing the cell death in breast cancer cells through the activation of EGFR signaling. Hence, EGFR overexpressed human breast cancer cells, MCF-7 and SkBr3 (NCCS, Pune, India) were chosen for the study. Cells cultured in DMEM medium, with 10% Fetal Bovine Serum, at 37 °C, 5% CO_2 in a humidified atmosphere. The non-cancerous cells, H9C2 (cardiomyocyte), were also maintained in the same medium as above. All the cell lines used in the study was EGFR (+).

2.2. Indoline derivatives

Seven indoline derivatives were selected for studying the anti-breast cancer effect and their mechanism of action. The list of selected compounds as follows: *N*-(2-hydroxy-5-nitrophenyl(4′-methylphenyl)methyl)indoline (HNPMI); (2-(3,4-dihydroquinolin1(2H)-yl)(p-tolyl)methyl)phenol); 2-(indolin-1-yl(4-methoxyphenyl)methyl)phenol; 2-(indolin-1-yl(4-methoxyphenyl)methyl)-4-nitrophenol; 2-(indolin-1-yl (phenyl)methyl)-4-nitrophenol; 2-(indolin-1-yl(phenyl)methyl)-4-nitrophenol; 2-(indolin-1-yl(p-tolyl)methyl)-4-nitrophenol.

2.3. Virtual screening and synthesis of chemical compounds

Molecular docking was performed to identify the best potent inhibitor of EGFR among the seven indoline derivatives using *i*GEMDOCK (Hsu et al., 2011). The seven indoline structures were drawn using ACD/Chemsketch (Fig. 1A) (Hunter, 1997). The structures were cleaned and energy minimization was done using Frog2 online tool (Leite et al., 2007). The EGFR structure was retrieved from PDB database and its active site residues were identified. The interaction profiles was analyzed for these ligands and the interaction poses were visualized using Pymol (Schrödinger, 2015). AEE788 (Traxler et al., 2004) and Gefitinib (Pao et al., 2004), an EGFR inhibitor(s) were used as a reference compounds. From the docking score, the compound (HNPMI) with the lowest binding energy was chosen for the synthesis. The compound HNPMI was synthesized (Fig. 1D) using the salicylaldehyde as the carbonyl component in the Petasis-borono Mannich reaction in glycerol at 50 °C by a previously established methodology (Rosholm et al., 2015) starting from salicylaldehyde and the corresponding boronic acid. After the completion of the reaction, good yield of HNPMI was obtained by flash chromatography by diluting the reaction media with water and saturated $NaHCO_3$ solution and finally extracted with diethyl ether. Despite the mass transfer issues in reactions observed in high viscosity glycerol, raising the reaction temperature to 50 °C or 80 °C was enough to ensure the formation of the desired compound after 24 h or 48 h. NMR characterization was performed as previously explained (Supplementary file: Spectral data) (Doan et al., 2016)and further used for in-vitro analysis.

2.4. RNA extraction and cDNA synthesis

MCF-7 and SkBr3 cells were grown as described above and once the cells reaches 75% confluence, they were treated with the IC_{50} concentration of HNPMI for 24 h. Total RNA from the untreated and HNPMI treated MCF-7 cells were extracted using One step-RNA Reagent (Biobasic Inc.). RNA was extracted, air dried and dissolved in DEPC water and used for cDNA synthesis. It was reverse transcribed with Easy Script Plus™ Reverse Transcriptase. For RT-PCR reaction, 1–2 μg of RNA and 2 μl of oligo-dT was incubated at 65 °C for 5 min and chilled immediately on ice. To this, 4 μlof 1X reverse transcriptase buffer, 2 μl of 2.5 mM dNTP mix, and 0.5 μl of RNase inhibitor (40 U/μL) were added and incubated for 5 min at 42 °C. To this mixture, 1 μl Easy Script reverse transcriptase (200 U/μL) was added and the reaction was left at 42 °C for 50 min followed by 70 °C for 10 min and chilled on ice.

2.5. RT-PCR analysis

The expression of target genes EGFR, PI3K, and S6K1 along with housekeeping gene, β-actin were analyzed using RT-PCR. The specific forward and reverse primers were used as follows: EGFR (F: 5′ TCCC CGTAATTATGTGGTGACAGATC 3′ and R: ACCCCTAAATGCCACCGGC 3′); *PI3K* (F: 5′ AACACAGAAGACCAATACTC 3′ and R: 5′ TTCGCCAT CTACCACTAC 3′); *S6K1* (F: 5′CACATAACCTGTGGTCTGTTGCTG 3′ and R: 5′ AGATGCAAAGCGAACTTGGGATA 3′); and *β-actin* (F: 5′ CACCCG CGAGTACAACCTT 3′ and R: 5′ CCCATACCCACCATCACACC 3′), were synthesized commercially and used for PCR. The PCR mixture contains 1X Taq Buffer (with $MgCl_2$), 0.2 mM dNTPs, 2.5 mM $MgCl_2$, 0.3 μM Forward and Reverse primers, template cDNA and 1U Taq Polymerase. The PCR cycle was set up as follows; Initial denaturation (94 °C - 2min), denaturation (94 °C −30s), annealing (Ta-1min), extension (72 °C - 1min 20s), final extension (72 °C - 7min) and hold at 4 °C. The cycle was repeated for 32 times. Ta for β-actin- 54 °C; EGFR – 56 °C; PI3K – 54 °C; S6K1 - 56 °C. After the reaction, the products were separated on 1.5% agarose gel. 100bp DNA ladder was used for reference. The gene expression was quantified by measuring the intensity of the DNA band using the ImageJ program.

2.6. Cell viability/proliferation assay

The cell cytotoxicity was measured using MTT assay in all three cell lines (Mosmann, 1983). Briefly, the cells were plated in 96 well plates with a cell density of approximately 1.2×10^4 cells/well. At 70% confluence, the cells were treated with varying concentrations of HNPMI (10, 25, 50, 75, and 100 μM). Untreated cells were also maintained as a control. After 24 h of incubation, 10μlof MTT (5 mg/ml) was added and incubated for 4 h at 37 °C. 100 μl of DMSO was added to dissolve the formazan crystals that are formed, and the absorbance was read at 570 nm in a microtiter plate reader. Cyclophosphamide was used as a positive control (Bang et al., 2000; Mamounas et al., 2005). Dose response curve was plotted to calculate the IC_{50} concentration using concentration-effect curve function of Graphpad Prism 6. Three technical and biological repeats were performed for each condition and the data are presented as mean of 3 independent ± standard error of the mean.

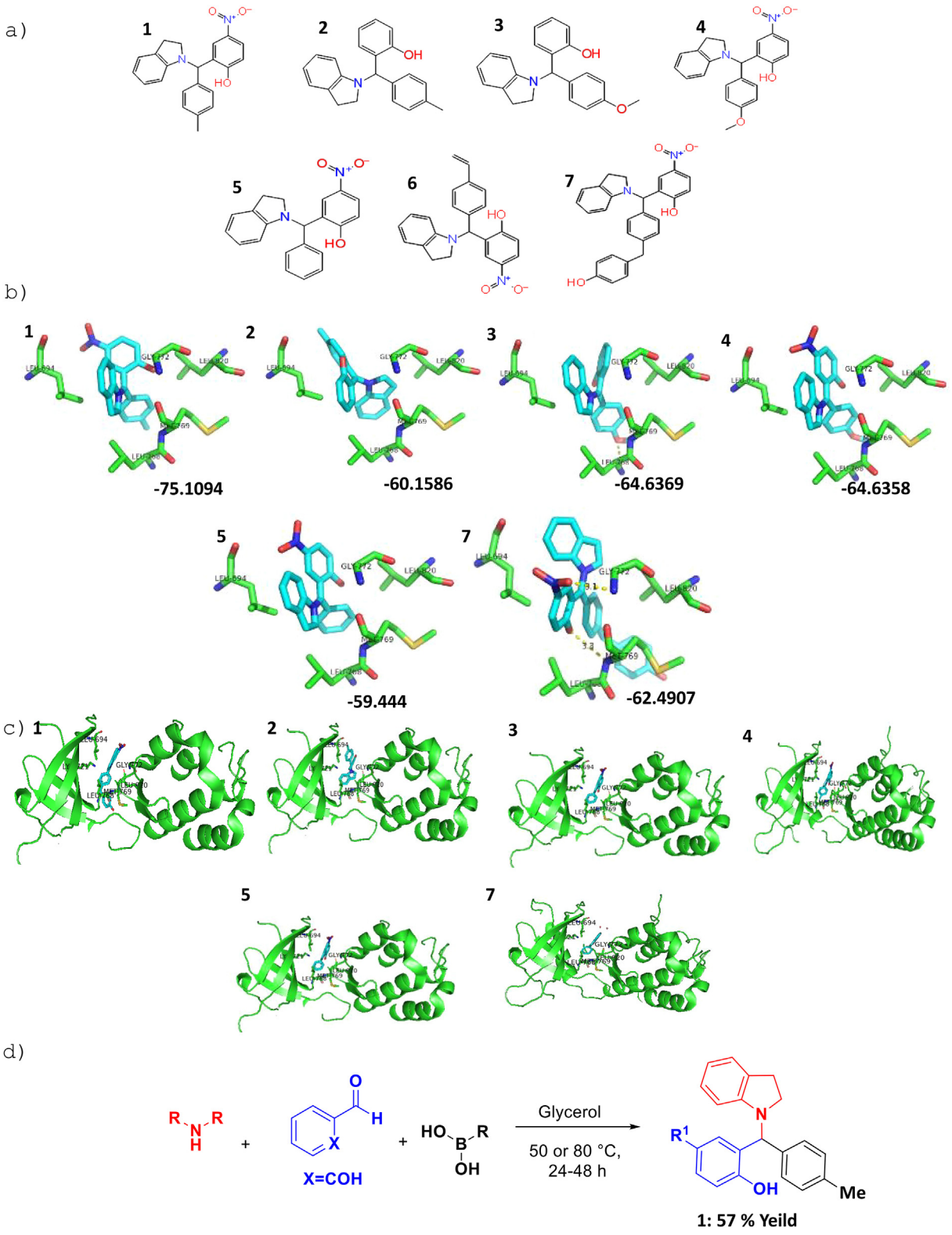


Fig. 1. Compound structure and their interaction with EGFR (A) 2D structure of indoline derivatives (B) Molecular docking analysis of indoline derivatives with EGFR. The surface-docking model of HNPMI in the EGFR active site. The docking score is represented for each model. The ligand is represented as sticks; and the protein active sites are represented as lines. Hydrogen bond interaction are shown in dotted lines (Red) and the interacting residues are labelled (C) Ligand-receptor interaction (D)Synthesis of top ligand, N-(2-hydroxy-5-nitrophenyl(4′-methylphenyl) methyl) indoline HNPMI. (For interpretation of the references to color in this figure legend, the reader is referred to the Web version of this article.)

Table 1
List of Training set and Test set of compounds used for QSAR model.

Training Set			
S.No	Compound Name	IC_{50} (μM)	References
1	N-(2-hydroxy-5-nitrophenyl(4′-methylphenyl)methyl)indoline	64.10	Present Study
2	TAMOXIFEN	6,05	Mokhtari et al. (2012)
3	4-((5-bromo-2-oxoindolin-3-ylidene)methyl)benzonitrile	6	
4	N-(2-fluoro-4-((2-oxoin dolin-3-ylidene) methyl)phenyl)acetamide	9,3	
5	3-(4-((4-methylpiperazin-1-yl)methyl)benzylidene)indolin-2-one	42,07	
6	3-((5-(4-fluorophenyl)pyridin-3-yl)methylene)indolin-2-one	8,54	
7	4-(2-oxo-5-(trifluoromethoxy)indolin-3-ylideneamino)benzamide	27,2	
8	4-(5, 7-dichloro-2-oxoindolin-3-ylideneamino)benzamide	65,86	
9	7-(Hy d roxymethy l ene) - 2 - m e t hy l - 5, 7, 8, 9, 1 0, 1 1 -hexahydrocycloocta[b]indol-6-one	27,34	Vairavelu and Prasad KJ (2016))
10	2-C hl or o - 7 - (hy d roxymethy l e n e) - 5, 7, 8, 9, 1 0, 1 1 -hexahydrocycloocta[b]indol-6-one	21,96	
11	7-(Hy d roxymethy l ene) - 4 - m e t hy l - 5, 7, 8, 9, 1 0, 1 1 -hexahydrocycloocta[b]indol-6-one	37,79	
12	7-(Hydroxymethylene)-5,7,8,9,10,11-hexahydrocycloocta[b] indol-6-one	49,45	
13	9-Methyl-4,5,6,7-tetrahydropyrazolo[3′,4':8,7]-12Hcycloocta[b]indole	30,41	
14	9-Chloro-4,5,6,7-tetrahydropyrazolo[3′,4':8,7]-12Hcycloocta[b]indole	15,98	
15	11-Methyl-4,5,6,7-tetrahydropyrazolo[3′,4':8,7]-12Hcycloocta[b]indole	35,77	
16	4,5,6,7-Tetrahydropyrazolo[3′,4':8,7]-12H- cycloocta[b]indole	47,56	
17	9-Methyl-4,5,6,7-tetrahydroisoxazolo[3′,4':8,7]-12Hcycloocta[b]indole	29,96	
18	9-Chloro-4,5,6,7-tetrahydroisoxazolo[3′,4':8,7]-12Hcycloocta[b]indole	21,96	
19	11-Methyl-4,5,6,7-tetrahydroisoxazolo[3′,4':8,7]-12Hcycloocta[b]indole	37,14	
20	4,5,6,7-Tetrahydroisoxazolo[3′,4':8,7]-12H-cycloocta[b]indole	48,26	
21	9-Methyl-1-phenyl-4,5,6,7-tetrahydropyrazolo[3′,4':8,7]-12Hcycloocta[b]indole	50,41	
Test Set			
S.No	**Compound Name**	**IC_{50} (μM)**	**References**
1	9-Chloro-1-phenyl-4,5,6,7-tetrahydropyrazolo[3′,4':8,7]-12Hcycloocta[b]indole	27.23	Vairavelu and Prasad KJ (2016)
2	11-Methyl-1-phenyl-4,5,6,7-tetrahydropyrazolo[3′,4':8,7]-12Hcycloocta[b]indole	25.22	
3	1-Phenyl-4,5,6,7-tetrahydropyrazolo[3′,4':8,7]-12Hcycloocta[b]indole	54.61	
4	2-Hydroxy-10-methyl-5,6,7,8-tetrahydropyrimido[5′,6':8,7]-13H-cycloocta[b]indole	30.13	
5	2-Hydroxy-10-chloro-5,6,7,8-tetrahydropyrimido[5′,6':8,7]-13Hcycloocta[b]indole	11	
6	2-Hydroxy-12-methyl-5,6,7,8-tetrahydropyrimido[5′,6':8,7]-13H-cycloocta[b]indole	32	
7	2-hydroxy-5,6,7,8-tetrahydropyrimido[5′,6':8,7]-13H-cycloocta[b]indoles	45	
8	2-Mercapto-10-methyl-5,6,7,8-tetrahydropyrimido[5′,6':8,7]-13H-cycloocta[b]indole	31	
9	2-Mercapto-10-chloro-5,6,7,8-tetrahydropyrimido[5′,6':8,7]-13H-cycloocta[b]indole	12.35	
10	2-Mercapto-12-methyl-5,6,7,8-tetrahydropyrimido[5′,6':8,7]-13H-cycloocta[b]indole	34	
11	2-Mercapto-5,6,7,8-tetrahydropyrimido[5′,6':8,7]-13Hcycloocta[b]indole	46	

2.7. Caspases 3 and caspases 9 activity assays

Drug induced cell apoptosis was measured by estimating caspase-3 and caspase-9 level by chromogenic assays following the manufacturer's protocol (Calbiochem, Merck). The MCF-7 and SkBr3 were treated with HNPMI for 24 h and lysed using Lysis buffer (50 mM HEPES, 100 mM NaCl, 0.1% CHAPS, 1 mM DTT, 100 mM EDTA). The cytosolic extracts were collected by centrifugation of the lysate, and the concentration of the protein was determined by Bradford assay using BSA as a standard. To each reaction sample 50 μl of cell lysate containing 100–200 μg of total protein was added. Cellular extracts were incubated with 5 μl of the 4 mM p-nitroanilide (pNA) substrates, DEVD-pNA (caspase- 3 activity) for 2 h at 37 °C. The amount of free pNA was calculated by measuring the absorbance cleaved substrates at 405 nm in a plate reader. Relative Caspase-3 and 9 activities were calculated based on the absorbance of free pNA from treated cells to untreated cells.

2.8. DNA isolation and agarose gel electrophoresis

The DNA fragmentation analysis was performed in MCF-7 cell line in order validate the apoptosis using gel electrophoresis (Basnakian and James, 1994). MCF-7 cells were grown in appropriate culture medium and at 75% confluence the cells were treated with IC_{50} concentration of HNPMI for 24 h. The HNPMI treated and control cells were lysed using lysis buffer. After incubation and centrifugation, phenol: chloroform: isoamylalcohol mixture was added to the supernatant to spool out DNA in the aqueous phase. DNA was precipitated using ammonium acetate and ice-cold isopropanol. After a repeated wash with 70% ethanol, the isolated DNA was stored in 20–50 μl of TE buffer. Samples were loaded in 2% agarose gel (w/v) and run at 50 V. DNA Ladder Mix (1 kb) was used as marker and DNA was detected using ethidium bromide under UV transilluminator.

2.9. Fluorescence activated cell sorting analysis

Translocation of membrane phosphatidylserine (PS) is a phospholipid which is translocated from the internal plasma membrane to the surface of the lipid layer is the hallmark in identifying apoptotic cells. Annexin V is a phospholipid-binding protein that has high affinity for PS. The fluorochrome-labelled Annexin V was used for the detection of translocated PS using Fluorescence activated cell sorting (FACS). The induction of apoptosis in MCF-7 cell line after the treatment with HNPMI was determined by FACS analysis(Vermes et al., 1995). MCF-7 cells at the confluence of 75% were treated with HNPMI in three different concentrations viz. 59.10 μM, 64.10 μM and 69.10 μM and the control well was left untreated. The cells were incubated for 24 h, trypsinised and the cell pellet was suspended in PBS. The cells were washed with 1X binding buffer at a concentration of 1×10^6 cells/ml. To this suspension, 5 μl of FITC Annexin V and 5 μl propidium iodide were added and vortexed gently. Cells were further incubated at 25 °C for 15 min in dark. Treated and control cells were mixed with 400 μl of 1X Binding Buffer and the apoptotic cell were analyzed by flow cytometry within 1 h.

2.10. Acridine orange/ethidium bromide dual staining

Dual staining was performed in MCF-7 cells to visualize the potential of the HNPMI induced apoptosis. MCF-7 cells were grown on six

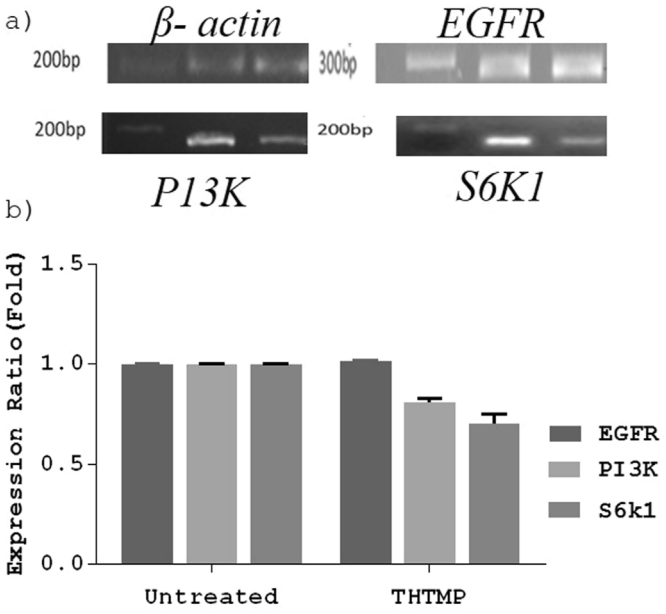


Fig. 2. Gene expression analysis of EGFR downstream signaling genes. (A) PCR amplification of β-actin (204bp), EGFR (250bp), P13K (195bp) and S6K1 genes (180bp). (Lane 1: 100bp DNA marker, Lane 2: Control (Untreated) (B) Optical density was measured to determine the fold change of mRNA expression for EGFR, S6K1, and PI3K genes, normalised with the housekeeping gene β-actin.

well plates and treated with three different concentrations (59.10 μM, 64.10 μM and 69.10 μM) of HNPMI for 24 h and control well was left untreated. The cells were trypsinised and suspended in PBS. Staining solution (1:1) mixture of 100 μg/ml AO and 100 μg/ml EB were added to this solution and 10 μl suspension was placed on a clean microscopic slide and observed under a fluorescent microscope with a blue filter (420–495 nm) and a green filter (510–560 nm). The cells were viewed in different fields and quantified using 300 cells per well(Basikc et al., 2006).

2.11. QSAR analysis of HNPMI

The relationship between the molecular descriptors of the set of compounds of interest with their respective biological activity has been studied by using quantitative structure-biological activity/property relationship (QSAR)(Roy et al., 2015). In this study, a QSAR approach was performed quantitatively to depict and provide mechanistic insights into interactions between the chemical structures of HNPMI by considering the compounds with similar structures.

In this analysis, 32 compounds were selected those shares significant similarity with the HNPMI. Since there are very limited experimentally confirmed compounds for the target, tamoxifen (Mokhtari et al., 2012), a non-indoline derivative is also has been selected for the QSAR analysis. The total of 32 compounds and their biological activity in terms of IC_{50} were chosen from the literature (Table 1). The descriptors for the compounds was calculated using Dragon software. The Dragon software was classified into 18 groups from 1497 descriptors. DRAGON software was used to calculate the set of 18 descriptors for each molecule in the training set (Todeschini et al., 2009). To most relevant set of descriptors was selected based on the IC_{50} of the compounds, and the MLR models were built. BUILDQSAR software was used to eliminate the variables. The goodness of the correlation was assessed by the square of coefficient regression (R^2), square of cross regression (q^2), the F-test (F), and the standard deviation (Std). The number of compounds is represented as “n” and the correlation coefficient as “r”.

2.12. Prediction of ADMET properties

A computational study of synthesized compound HNPMI was performed to predict the ADMET properties. ADMET filtering was done using admetSAR (http://www.admetexp.org/predict/). We assessed drug likeliness properties that signify the compound with good Absorption, Distribution, Metabolism, Excretion and Toxicity of HNPMI in breast cancer treatment.

3. Results

3.1. HNPMI interaction with EGFR and its downstream signaling effect on breast cancer cells

The aim of the study was to elucidate the interaction of seven indoline derivatives with EGFR protein (Fig. 1A). Molecular docking was employed to understand the binding affinity of active sites of EGFR protein with the selected indoline derivatives. The crystallographic 3D structure of EGFR protein was downloaded from Protein Databank (PDB ID:1M17) with a resolution of 2.6 Å, that served as a template. The active site residues of EGFR protein were found as follow, Lys-721, Met-769, Leu-768, Leu-820, Pro-770, Leu-694 and Gly-772. Also, the ligands structure was drawn using Chemsketch and saved as.mol file. The molecular docking studies was performed using iGEMdock (version 2.1). Docking of selected seven ligands against EGFR active site revealed the binding efficiency of six ligands except the compound “2-(indolin-1-yl(phenyl)methyl)-4-nitrophenol” with the nil docking pose (Fig. 1B). The ligand receptor interaction is represented in Fig. 1C. The compound, HNPMI showed strong binding behavior among all the tested compounds against the EGFR with the minimum binding energies −75.104 kcal/mol. Molecular docking disclosed the interaction of HNPMI with EGFR receptor through the hydrogen bonding and charged residue interactions with 29 amino acids. The results revealed that in HNPMI, the ligand – receptor (EGFR) complex exhibits two hydrogen bonds, one with amino acid Gly772 and the other with amino acid Met769. Also, to validate the binding efficiency of HNPMI, reference compounds such as AEE788 and Gefitinib were also docked with the target protein, EGFR (Supplementary file: Fig. 1A and B). The compound AEE788 exhibited the binding energy of −9.5 kcal/mol with the hydrogen bond interactions at Gln767, Met769, Thr766 whereas Gefitinib showed the binding energy of −7.9 kcal/mol with the hydrogen bond interactions at Met769, Thr830, Glu738. This data revealed that HNPMI exhibited least binding energy with highest docking score than the reference compounds, thus proving HNPMI as a potential target of EGFR and it was synthesized for further invitro analysis (Fig. 1D).

To better understand the effect of HNPMI in the EGFR downstream signaling pathway, the gene expression changes of EGFR, PI3K and S6K1 was performed by RT-PCR. Firstly, EGFR (250bp), PI3K (195bp), S6K1 (180bp) and the housekeeping gene, β-actin (180bp) were amplified using the cDNA of both the drug treated and control MCF-7 cells (Fig. 2A). Gene expression level was quantified using ImageJ tool using the gel image of amplicon (Fig. 2B). There is an alteration in the relative expression level of genes PI3K and S6K1, whereas the expression of EGFR doesn't show significant change in the cells treated with IC_{50} concentration of HNPMI when compared to the control cells. There is 0.4-fold decrease in the expression of S6K1 and 0.3-fold decrease for PI3K when compared with the control cells (Fig. 2B). Thus, the HNPMI downregulates the S6K1 and PI3K via EGFR signaling activation, which might possibly induce cell death.

3.2. Cytotoxicity of HNPMI

The cytotoxic activity of HNPMI (Fig. 3A) and cyclophosphamide (Fig. 3B) as a reference compound was investigated against breast cancer cell lines, MCF-7 and SkBr3 cell lines and non-cancerous (H9C2)

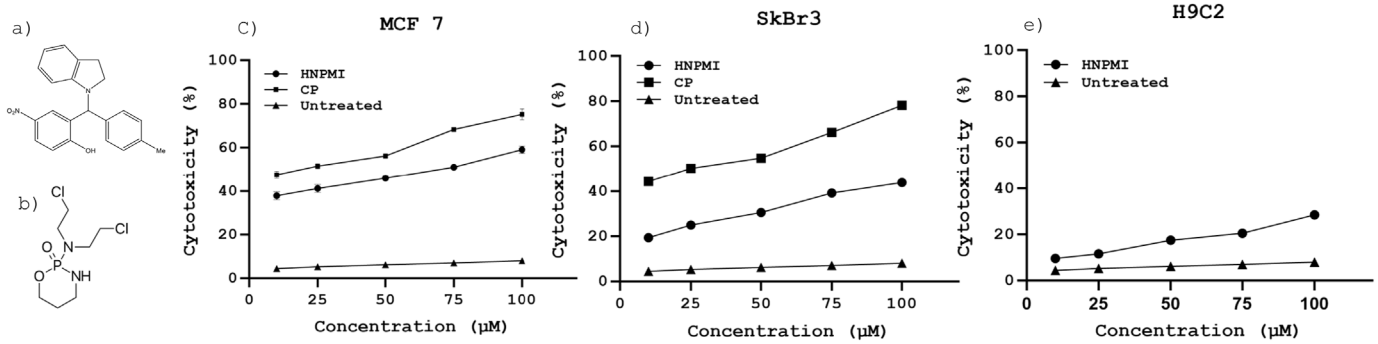


Fig. 3. Cytotoxicity effect of HNPMI in breast cancer and non-cancerous cells. (A) 2D structure of HNPMI and (B) Cyclophosphamide (CP, positive control). IUPAC: N-(2-hydroxy-5-nitrophenyl (4′-methylphenyl) methyl) indoline (M. wt – 329.443) and N, N-bis(2-chloroethyl)-2-oxo-1,3,2λ^{5}oxazaphosphinan-2-amine (M.wt.261.083) respectively, Dose dependent cytotoxicity effect of HNPMI and CP in breast cancer cells, MCF-7(C), SkBr3 (D) and H9C2 (non-cancerous cell), untreated (E). Error bar represents mean S.E.M. (n = 3 per group) with the statistical significance, p-values (*P < 0.05).

cell lines with varying concentration ranging from 10 to 100 μM. HNPMI have shown a dose-dependent reduction in the viability of these cells. The results show 33.96% and 50.93% cytotoxicity against MCF-7 cells whereas 14.64% and 39.07% toxicity for SkBr3 cells at 10 μM and 100 μM, respectively. HNPMI have the toxicity against MCF-7 (Fig. 3C) and SkBr3 (Fig. 3D) cell lines with IC_{50} values of 64.10 μM and 119.99 μM respectively. The IC_{50} value of the cyclophosphamide was found to be 21.37 μM in MCF7 and 38.34 μM in SkBr3. Interestingly, the HNPMI showed negligible level of cytotoxicity in non-cancerous cell, H9C2 when compared to the untreated cells (Fig. 3E).

3.3. Effects of HNPMI on caspases induction

The effect of anticancer drug on activation of caspase 3 and 9 is considered as the crucial in assessing the cytotoxicity. On treatment with HNPMI, MCF-7 and SkBr3 have shown an increased fold change of Caspase 3 and 9. At IC_{50} concentration, caspase 3 activity is elevated by a fold of 0.218 and 0.098 in MCF-7 and SkBr3, respectively (Fig. 4A), when compared to untreated cells. Similarly, caspase 9 activity has been increased by a fold of 0.478 and 0.269 in MCF-7 and SkBr3, respectively (Fig. 4B). The observed fold changes for both caspase 3 and 9 in treated conditions are statistically significant (*P ≤ 0.005) than the untreated condition.

3.4. HNPMI induces apoptosis mediated DNA fragmentation in MCF-7 cells

Caspase activation triggers cascade of downstream pathways that induces DNA fragmentation. To investigate the ability of HNPMI inducing apoptosis mediated cell death, the DNA laddering assay was performed. The DNA of the MCF-7 cells were exposed with IC_{50} concentration of HNPMI that leads to DNA fragmentation, whereas the untreated cells did not provide ladders of DNA (Fig. 5A). These results confirmed that HNPMI caused internucleosomal DNA fragmentation in the MCF-7 cells exhibiting the characteristic features of apoptosis causing cell death.

To gain more insight into the mode of action of apoptotic cell death by HNPMI, the phosphatidylserine externalization was detected by FACS. On treating MCF-7 cells with HNPMI for 24 h, around 54% of the cells were found to be viable, 1.06% cells are at early apoptotic cells, 39.61% of cells are at late apoptotic cells and 2.31% of cells are necrotic cells (Fig. 5B, C and D).

Induction of apoptosis was independently validated by AO/EtBr staining. The morphological evidences for apoptosis were also observed using dual staining. Apoptotic cells were marked by granular yellow-orange nuclear staining. The cells were characterized with nuclear shrinkage and blebbing of the nuclear membrane but in-contrast, necrotic cells showed uniform orange under fluorescent microscopy. The untreated cells appeared to have normal and green color nuclear staining (Fig. 6A-D). Dose dependent treatment with 59.10 μM, 64.10 μM and 69.10 μM HNPMI showed increased percentage of apoptosis of about 12%, 43% and 40% of apoptotic cells respectively (Fig. 6E). All the above observations suggested that HNPMI treatment induced apoptosis mediated cell death in MCF-7 cells.

3.5. Biological activity of HNPMI and its ADMET property

The anticancer activity of HNPMI was tested against the biological activity using built QSAR. The biological properties of the chemical molecules based on their chemical structure was analyzed. The QSAR model was built and the best compound which fits well with the model

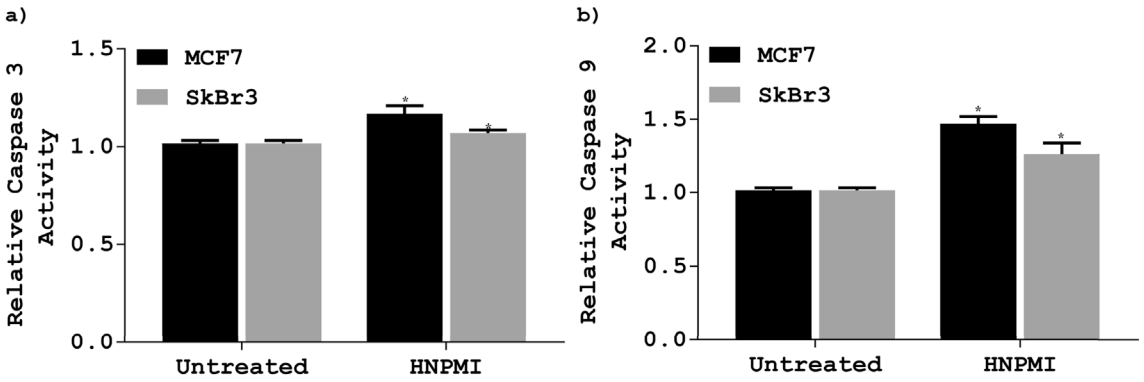


Fig. 4. Caspase 3 and Caspase 9 activity in breast cancer cells treated with IC_{50} concentration of HNPMI. (A) Relative caspase 3 activity of HNPMI in MCF7 cells and SKBr3 cells in treated and untreated conditions (B) relative caspase 9 activity as similar condition (A). Data represents mean ± S.E.M. of two individual experiments (n = 3 with the statistical significance, p-values (Two-way anova, *P ≤ 0.005).

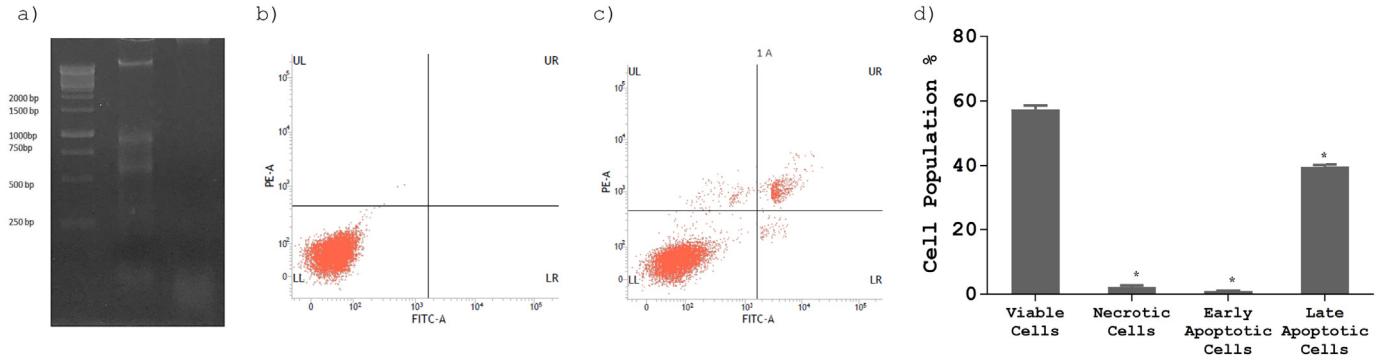


Fig. 5. Apoptosis induction in cells treated with IC_{50} concentration of HNPMI (A) 1.5% agarose gel electrophoresis of DNA extracted from HNPMI treated and untreated cells MCF-7 cells, Lane 1- 1 Kb Ladder; Lane 2 - DNA of cells treated with HNPMI; Lane 3- DNA of untreated cells. FACS assessment of cell apoptosis using Annexin/PI staining (B) untreated MCF-7 cells (C) HNPMI treated MCF-7 cells, UL- Necrotic cells, UR- Late apoptotic cells, LL - Viable cells, LR – Early apoptotic cells; (D) Percentage of cell population at different stages of cell death. Data represents mean ± S.E.M. of two individual experiments (n = 3 with the statistical significance, p-values (Two-way anova, *P ≤ 0.005).

was considered to show better biological activity when compared with the other compounds. Kennard-Stone algorithm was employed to divide the studied compounds, which comprised 32 compounds into a training set of 21 compounds and a test set of 11 compounds (Table 1). Multi-linear regression model was used to generate the QSAR model, in which the compounds were considered as outliers that has the significant deviation from the regression line. The correlation coefficient value (r) of the QSAR model was 0.947 and the test set value was 0.993 (Fig. 7) and this helps in predicting the anticancer activity of the QSAR model. The model generated using QSAR emphasized the presence of the indole ring, the aromaticity and certain other substituents like nitrogen and oxygen ascertain to the biological activity of the compounds.

From the ADMET analysis, it has been proven that HNPMI has good pharmacokinetic properties and obeyed the drug likeliness rules. The end points activity, calculated activities of the inhibitors and the accuracy value for each compound were reported in Table 2. The *in-silico* prediction of oral bioavailability and ADMET risk profiling are within their acceptable limit for HNPMI. It has good absorption properties, predicted to cross blood-brain barrier, CaCO-2 permeability and good intestinal absorption. It was predicted to be localized in mitochondria of the cell. The metabolism and toxicity parameters are also in acceptable limit for the compound. In terms of metabolism, it was found to act as a substrate and noninhibitor of CYP450. The compound by itself has no carcinogenicity property. The result elucidates that HNPMI has good drug likeliness property. Thus, HNPMI can be suggested as a to develop as a new drug candidate that possess unique ADMET properties.

4. Discussion

Indoline derivatives have gained importance as an anti-breast cancer drug and hence the synthesis of pharmacologically potential indoline derivatives is of immense interest in recent years. HNPMI is a novel indole derivatives characterized as a potent anticancer compound against bone cancer (Doan et al., 2017) and brain tumor (Doan et al., 2019). We have investigated the ability of the HNPMI to inhibit breast cancer cell proliferation and apoptosis induction in cancerous cells. Previously, indole derivates, diindolylmethanes flouro and cyano derivatives have cytotoxic effect towards tumor MCF7, NCI–H460, and SF-268 cells (Hong et al., 2002; Mousavi et al., 2011). HNPMI induced reduction in the cell viability of both cells, MCF-7 and SKBr3 without affecting the non-cancerous cells, H9C2 in a dose dependent manner.

The HNPMI used in the present study contains nitro group. Previous studies have reported the presence of nitro groups as a toxicophoric

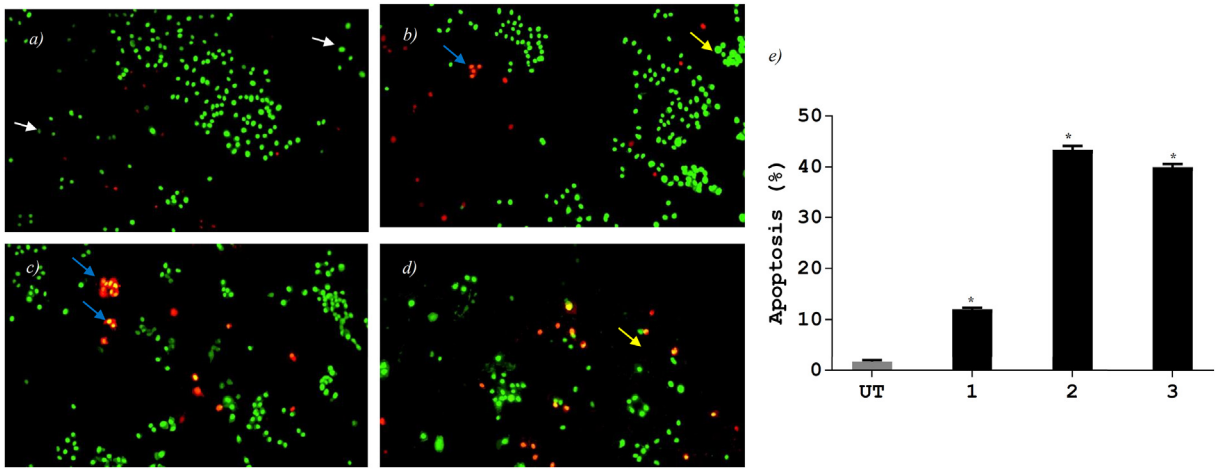


Fig. 6. Fluorescence microscopy images of AO-EtBr staining for deduction of apoptosis in. MCF7 cells (A) Untreated cells (B) MCF7 cells treated with 59.10 μM HNPMI (C) 64.10 μM (D) 69.10 μM. Appearance of green fluorescence (white arrow) in untreated control cells represents viable cells with normal morphology whereas visualization of bright yellow green color (yellow arrow) and reddish yellow/orange staining (blue arrow) in the treated cells shows the presence of early and late apoptotic cells. Necrotic cells appear a uniform orange stain; (E) percentage of. apoptosis in treated and untreated MCF-7 cells with different concentration of HNPMI where 1 is 59.10 μM; 2 is 64.10 μM; and 3 is 69.10 μM. Data represents mean ± S.E.M. of two individual experiments (n = 3 with the statistical significance, p-values (Two-way anova, *P ≤ 0.005). . (For interpretation of the references to color in this figure legend, the reader is referred to the Web version of this article.)

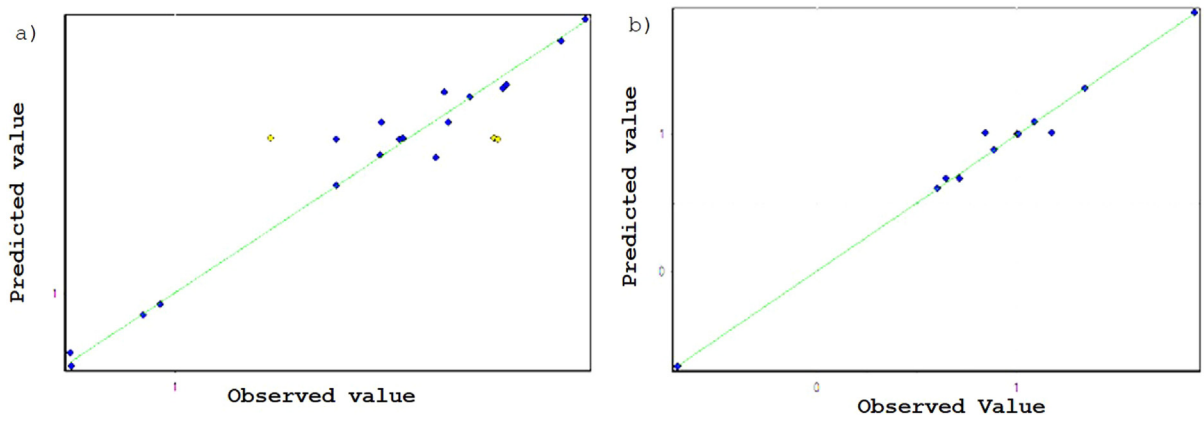


Fig. 7. Correlation of biological activity and physicochemical parameters of (A) training set (R2 = 0.947) and (B) test set (Q2 = 0.993).

Table 2
ADME properties of the ligand HNPMI.

Descriptor(s)	HTS Data	Accuracy
Blood-Brain Barrier	BBB+	0,8003
Human Intestinal Absorption	HIA+	0,9971
Caco-2 Permeability	Caco2+	0,5375
P-glycoprotein Substrate	Non-substrate	0,7583
P-glycoprotein Inhibitor	Non-inhibitor	0,6068
	Non-inhibitor	0,9278
Renal Organic Cation Transporter	Non-inhibitor	0,8148
Subcellular localization	Mitochondria	0,6819
CYP450 2C9 Substrate	Non-substrate	0,6246
CYP450 2D6 Substrate	Non-substrate	0,8092
CYP450 3A4 Substrate	Substrate	0,6311
CYP450 1A2 Inhibitor	Inhibitor	0,7358
CYP450 2C9 Inhibitor	Inhibitor	0,651
CYP450 2D6 Inhibitor	Non-inhibitor	0,8645
CYP450 2C19 Inhibitor	Non-inhibitor	0,5508
CYP450 3A4 Inhibitor	Non-inhibitor	0,7413
CYP Inhibitory Promiscuity	High CYP Inhibitory Promiscuity	0,7253
Human Ether-a-go-go-Related Gene	Strong inhibitor	0,5167
Inhibition	Non-inhibitor	0,7336
AMES Toxicity	AMES toxic	0,9402
Carcinogens	Non-carcinogens	0,6772
Fish Toxicity	High FHMT	0,9583
Tetrahymena Pyriformis Toxicity	High TPT	0,9846
Honey Bee Toxicity	Low HBT	0,513
Biodegradation	Not ready biodegradable	0,9604
Acute Oral Toxicity	Category III	0,7048
Carcinogenicity (Three-class)	Warning	0,4551

compound. However, extensive studies were conducted in exploring compounds containing nitro groups as anticancer agents, antitubercular agents, and antiparasitic agents. These compounds induce cell death by various mechanisms like topoisomerase inhibition, histone deacetylase inhibition, DNA alkylation, or tubulin polymerization inhibition, and have significantly demonstrated hypoxia-induced effects that are attributed to their bio-reductive activation potential. Some of the compounds are selectively toxic to bacteria, parasites, or tumor cells without harming the host organism or normal cells because of their nitroaromatic and heteroaromatic compounds(Nepali et al., 2019). In this aspect, our compound even though it bears nitro group, its cytotoxicity was higher in breast cancer cells than the non-cancerous cells.

Indole-based anticancer agents have been explored as a potential drug for regulating multiple signaling pathways of the cancer cells. Recently, a indole derivative, trisubstituted, shows cytotoxicity against MCF-7 cells by regulating MMP-2/MMP-9 molecule(Bakar et al., 2016). So far, the indole derivative Brassinin is shown to down-modulate the constitutive PI3K/Akt/mTOR in prostate cancer cells (Chripkova et al., 2014). Here, HNPMI was reported as a modulator of PI3K signaling pathway especially by downregulating S6K1 gene in breast cancer. Although, the HNPMI did not alter the expression of EGFR, it down-regulates the PI3K/S6K1 genes down the cascade.

Apoptosis represent one of the important features of malignant cells and majority of available anti-breast cancer drugs depends on the apoptosis induction. It was found that HNPMI have induced the apoptosis in MCF7 cells through DNA fragmentation. Previous studies on indole derivatives have also proven their role in cell death induction by apoptosis in MCF-7 cells (Weng et al., 2008). Also, PI3K genes are found to be overexpressed in the cancerous condition which prevents the cells entering apoptosis (Chikh et al., 2016). Here, HNPMI down-regulates the expression of these genes and stops the cells from entering cellular proliferation signaling pathway and also induces the apoptosis. ADMET analysis has also been performed to prove the compound's structural feature as suitable drug candidate. The relative analysis of QSAR model exhibits a strong harmonization in the biological activity and the physicochemical property of the compound. Overall, these results suggest that the HNPMI have potential effect against the growth of breast cancer cells through the apoptosis induction, which can be subjected to pre-clinical trials for breast cancer treatment.

5. Conclusion

Our results conclude that the HNPMI induce caspase mediated apoptosis through EGFR mediated downstream signaling pathway. HNPMI downregulates the S6K1 and PI3K via EGFR signaling activation. HNPMI act as a potential anti-breast cancer compound, which inhibits the growth of MCF-7 and SkBr3 cells without affecting the non-cancerous cells. QSAR further supports the quantitative structural relationship with it is biological significance. Also, considering the long-term administration of this drug as an anti-breast cancer agent, its excellent safety profile has been proved using ADMET studies. Overall, HNPMI is a promising candidate for executing further phase clinical trials with pharmacological importance for the treatment of breast cancer.

Ethical approval

This article does not contain any studies with human participants performed by any of the authors.

Compliance with ethical standards

The authors declare that they have no conflict of interest.

CRediT authorship contribution statement

Suresh Palanivel: Data curation, Formal analysis, Writing - original

draft. **Akshaya Murugesan:** Formal analysis, Data curation, Writing - review & editing. **Kumar Subramanian:** Data curation, Formal analysis. **Olli Yli-Harja:** Project administration, Writing - review & editing. **Meenakshisundaram Kandhavelu:** Conceptualization, Project administration, Investigation, Writing - review & editing.

Acknowledgement

We would like to thank Prof. Nuno R. Candeias, Faculty of Engineering and Natural Sciences, Tampere University for gift of synthesized compounds.

Appendix A. Supplementary data

Supplementary data to this article can be found online at https://doi.org/10.1016/j.ejphar.2020.173195.

References

Age Standardized (World) Incidence Rates, Breast, All Ages.
Ali, R., Wendt, M.K., 2017. The paradoxical functions of EGFR during breast cancer progression. Signal Transduct. Target. Ther. 2, 16042. https://doi.org/10.1038/sigtrans.2016.42.
Bakar, F., Kilic-Kurt, Z., Caglayan, M.G., Olgen, S., 2016. The effects of 1,3,5-trisubstituted indole derivatives on cell growth, apoptosis and MMP-2/9 mRNA expression of MCF-7 human breast cancer cells. Anticancer. Agents Med. Chem. 17, 762–767. https://doi.org/10.2174/1871520616666160802115737.
Bang, S.M., Heo, D.S., Lee, K.H., Byun, J.H., Chang, H.M., Noh, D.Y., Choe, K.J., Bang, Y.J., Kim, S.R., Kim, N.K., 2000. Adjuvant doxorubicin and cyclophosphamide versus cyclophosphamide, methotrexate, and 5-fluorouracil chemotherapy in premenopausal women with axillary lymph node positive breast carcinoma: results of a randomized controlled trial. Cancer. https://doi.org/10.1002/1097-0142(20001215)89:12<2521::AID-CNCR2>3.0.CO;2-F.
Basikc, D., Papovic, S., Ristic, P., Arsenijevic, N., 2006. Analysis of cycloheximide-induced apoptosis in human leukocytes: fluorescence microscopy using annexin V/propidium iodide versus acridin orange/ethidium bromide. Cell Biol. Int. 30, 924–932. https://doi.org/10.1016/j.cellbi.2006.06.016.
Basnakian, A.G., James, S.J., 1994. A rapid and sensitive assay for the detection of DNA fragmentation during early phases of apoptosis. Nucleic Acids Res. 22, 2714–2715.
Chikh, A., Ferro, R., Abbott, J.J., Piñeiro, R., Buus, R., Iezzi, M., Ricci, F., Bergamaschi, D., Ostano, P., Chiorino, G., Lattanzio, R., Broggini, M., Piantelli, M., Maffucci, T., Falasca, M., 2016. Class II phosphoinositide 3-kinase C2β regulates a novel signaling pathway involved in breast cancer progression. Oncotarget. https://doi.org/10.18632/oncotarget.7761.
Chripkova, M., Drutovic, D., Pilatova, M., Mikes, J., Budovska, M., Vaskova, J., Broggini, M., Mirossay, L., Mojzis, J., 2014. Brassinin and its derivatives as potential anticancer agents. Toxicol. Vitro 28, 909–915. https://doi.org/10.1016/J.TIV.2014.04.002.
Doan, P., Karjalainen, A., Chandraseelan, J.G., Sandberg, O., Yli-Harja, O., Rosholm, T., Franzen, R., Candeias, N.R., Kandhavelu, M., 2016. Synthesis and biological screening for cytotoxic activity of N-substituted indolines and morpholines. Eur. J. Med. Chem. 120, 296–303. https://doi.org/10.1016/j.ejmech.2016.05.024.
Doan, P., Musa, A., Candeias, N.R., Emmert-Streib, F., Yli-Harja, O., Kandhavelu, M., 2019. Alkylaminophenol induces G1/S phase cell cycle arrest in glioblastoma cells through p53 and cyclin-dependent kinase signaling pathway. Front. Pharmacol. https://doi.org/10.3389/fphar.2019.00330.
Doan, P., Nguyen, T., Yli-Harja, O., Candeias, N.R., Kandhavelu, M., 2017. Effect of alkylaminophenols on growth inhibition and apoptosis of bone cancer cells. Eur. J. Pharmaceut. Sci. 107, 208–216. https://doi.org/10.1016/j.ejps.2017.07.016.
Downward, J., Parker, P., Waterfield, M.D., n.d. Autophosphorylation sites on the epidermal growth factor receptor. Nature 311, 483–485.
Hong, C., Firestone, G.L., Bjeldanes, L.F., 2002. Bcl-2 family-mediated apoptotic effects of 3,3′-diindolylmethane (DIM) in human breast cancer cells. Biochem. Pharmacol. https://doi.org/10.1016/S0006-2952(02)00856-0.
Hsu, K.-C., Chen, Y.-F., Lin, S.-R., Yang, J.-M., 2011. iGEMDOCK: a graphical environment of enhancing GEMDOCK using pharmacological interactions and post-screening analysis. BMC Bioinf. 12, S33. https://doi.org/10.1186/1471-2105-12-S1-S33.
Hunter, A.D., 1997. ACD/ChemSketch 1.0 (freeware); ACD/ChemSketch 2.0 and its tautomers, dictionary, and 3D plug-ins; ACD/HNMR 2.0; ACD/CNMR 2.0. J. Chem. Educ. 74, 905. https://doi.org/10.1021/ed074p905.
Karjalainen, A., Doan, P., Chandraseelan, J.G., Sandberg, O., Yli-Harja, O., Candeias, N.R., Kandhavelu, M., 2018. Synthesis of phenol-derivatives and biological screening for anticancer activity. Anticancer. Agents Med. Chem. 17, 1710–1720. https://doi.org/10.2174/1871520617666170327142027.
Leite, T.B., Gomes, D., Miteva, M.A., Chomilier, J., Villoutreix, B.O., Tuffery, P., 2007. Frog: a FRee Online druG 3D conformation generator. Nucleic Acids Res. 35, W568–W572. https://doi.org/10.1093/nar/gkm289.
Mamounas, E.P., Bryant, J., Lembersky, B., Fehrenbacher, L., Sedlacek, S.M., Fisher, B., Wickerham, D.L., Yothers, G., Soran, A., Wolmark, N., 2005. Paclitaxel after doxorubicin plus cyclophosphamide as adjuvant chemotherapy for node-positive breast cancer: results from NSABP B-28. J. Clin. Oncol. https://doi.org/10.1200/JCO.2005.10.517.
Masuda, H., Zhang, D., Bartholomeusz, C., Doihara, H., Hortobagyi, G.N., Ueno, N.T., 2012. Role of epidermal growth factor receptor in breast cancer. Breast Canc. Res. Treat. 136, 331–345. https://doi.org/10.1007/s10549-012-2289-9.
Mokhtari, S., Mosaddegh, M., Hamzeloo Moghadam, M., Soleymani, Z., Ghafari, S., Kobarfard, F., 2012. Synthesis and cytotoxic evaluation of novel 3-substituted derivatives of 2-indolinone. Iran. J. Pharm. Res. IJPR 11, 411–421.
Mosmann, T., 1983. Rapid colorimetric assay for cellular growth and survival: application to proliferation and cytotoxicity assays. J. Immunol. Methods 65, 55–63.
Mousavi, S.H., Moallem, S.A., Mehri, S., Shahsavand, S., Nassirli, H., Malaekeh-Nikouei, B., 2011. Improvement of cytotoxic and apoptogenic properties of crocin in cancer cell lines by its nanoliposomal form. Pharm. Biol. https://doi.org/10.3109/13880209.2011.563315.
Musa, A., Tripathi, S., Kandhavelu, M., Dehmer, M., Emmert-Streib, F., 2018. Harnessing the biological complexity of Big Data from LINCS gene expression signatures. PloS One. https://doi.org/10.1371/journal.pone.0201937.
Nepali, K., Lee, H.Y., Liou, J.P., 2019. Nitro-group-containing drugs. J. Med. Chem. https://doi.org/10.1021/acs.jmedchem.8b00147.
Palanivel, S., Murugesan, A., Yli-Harja, O., Kandhavelu, M., 2020a. Anticancer activity of THMPP: downregulation of PI3K/S6K1 in breast cancer cell line. Saudi Pharmaceut. J. https://doi.org/10.1016/j.jsps.2020.02.015.
Palanivel, S., Yli-Harja, O., Kandhavelu, M., 2020b. Alkylamino phenol derivative induces apoptosis by Inhibiting EGFR Signaling Pathway in Breast Cancer Cells. Anticancer. Agents Med. Chem. https://doi.org/10.2174/1871520620666200213101407.
Pao, W., Miller, V., Zakowski, M., Doherty, J., Politi, K., Sarkaria, I., Singh, B., Heelan, R., Rusch, V., Fulton, L., Mardis, E., Kupfer, D., Wilson, R., Kris, M., Varmus, H., 2004. EGF receptor gene mutations are common in lung cancers from "never smokers" and are associated with sensitivity of tumors to gefitinib and erlotinib. Proc. Natl. Acad. Sci. U.S.A. https://doi.org/10.1073/pnas.0405220101.
Rosholm, T., Gois, P.M.P., Franzen, R., Candeias, N.R., 2015. Glycerol as an efficient medium for the Petasis borono-mannich reaction. ChemistryOpen 4, 39–46. https://doi.org/10.1002/open.201402066.
Roy, K., Kar, S., Das, R.N., Roy, K., Kar, S., Das, R.N., 2015. Validation of QSAR models. Underst. Basics QSAR Appl. Pharm. Sci. Risk Assess. 231–289. https://doi.org/10.1016/B978-0-12-801505-6.00007-7.
Schrödinger, L.L.C., 2015. The {AxPyMOL} Molecular Graphics Plugin for {Microsoft PowerPoint}, vol. 8 Versioñ1.
Todeschini, R., Consonni, V., Todeschini, R., 2009. Wiley InterScience (Online service). Molecular Descriptors for Chemoinformatics. Wiley-VCH.
Tong, C.W.S., Wu, M., Cho, W.C.S., To, K.K.W., 2018. Recent advances in the treatment of breast cancer. Front. Oncol. 8, 227. https://doi.org/10.3389/fonc.2018.00227.
Traxler, P., Allegrini, P.R., Brandt, R., Brueggen, J., Cozens, R., Fabbro, D., Grosios, K., Lane, H.A., McSheehy, P., Mestan, J., Meyer, T., Tang, C., Wartmann, M., Wood, J., Caravatti, G., 2004. AEE788: a dual family epidermal growth factor receptor/ErbB2 and vascular endothelial growth factor receptor tyrosine kinase inhibitor with antitumor and antiangiogenic activity. Canc. Res. https://doi.org/10.1158/0008-5472.CAN-03-3681.
Vairavelu, Leena, Prasad KJ, Rajendra, 2016. An expedient general synthesis of quinolino and pyrrolocycloocta[b]indoles. Organic Chem. Curr. Res. 5 (2), 1–4. https://doi.org/10.4172/2161-0401.1000165.
Vaiyapuri, P.S., Ali, A.A., Mohammad, A.A., Kandhavelu, J., Kandhavelu, M., 2015. Time lapse microscopy observation of cellular structural changes and image analysis of drug treated cancer cells to characterize the cellular heterogeneity. Environ. Toxicol. https://doi.org/10.1002/tox.21950.
Vermes, I., Haanen, C., Steffens-Nakken, H., Reutelingsperger, C., 1995. A novel assay for apoptosis. Flow cytometric detection of phosphatidylserine expression on early apoptotic cells using fluorescein labelled Annexin V. J. Immunol. Methods 184, 39–51.
Weng, J.-R., Tsai, C.-H., Kulp, S.K., Chen, C.-S., 2008. Indole-3-carbinol as a chemopreventive and anti-cancer agent. Canc. Lett. 262, 153–163. https://doi.org/10.1016/j.canlet.2008.01.033.